

Absorption and reduced scattering coefficient estimation in pigmented human skin tissue by experimental colorimetric fitting

LUISMAR B. CRUZ JUNIOR,^{1,*} CARLOS E. GIRASOL,² PEDRO S. COLTRO,³
RINALDO R. J. GUIRRO,² AND LUCIANO BACHMANN¹

¹Laboratory of Phobiophysics, Department of Physics, University of São Paulo, Ribeirão Preto, Brazil

²Laboratory of Physiotherapeutic Resources, Department of Health Sciences, University of São Paulo, Ribeirão Preto, Brazil

³Division of Plastic Surgery, Ribeirão Preto Medical School, University of São Paulo, Ribeirão Preto, Brazil

* contato.luismarjr@gmail.com

Received 22 March 2023; revised 19 July 2023; accepted 20 July 2023; posted 20 July 2023; published 0 MONTH 0000

This study aims to estimate the optical properties, absorption (μ_a), and reduced scattering (μ'_s) coefficients of *ex vivo* human skin through the individual typology angle (ITA) by only using the skin color parameters. Human skin samples were grouped according to their ITA value and measured using a colorimeter for validation. An integrating sphere and the inverse adding-doubling algorithm was applied to compute the samples μ_a and μ'_s . The μ_a increases as the ITA decreases. An axis swap was performed to generate the μ_a versus the ITA for all wavelengths between 500 nm and 800 nm with a spectral resolution of 10 nm. Linearization was performed and a correlation was found. An equation to fit μ_a based solely on the ITA values was estimated. The μ'_s does not change with ITA, but it could be fit with an inverse power law as a function of the wavelength. Both equations have a coefficient of determination (R^2) higher than 0.93, indicating a good agreement with our model. An experimental model to estimate the absorption and reduced scattering coefficients of *ex vivo* human skin through ITA was found. The model has high agreement with the experimental data, with an R^2 between 0.932 and 0.997, and these findings may be relevant for photobiomodulation and light treatment applications to estimate the effect of the melanin on the therapy. © 2023 Optica Publishing Group

<https://doi.org/10.1364/JOSAA.489892>

1. INTRODUCTION

Biophotonics devices are an important asset for human health. However, the effect of pigmentation on treatments and diagnoses still needs further investigation. It has been reported that higher concentrations of melanin in the skin may affect the response of optical techniques, such as pulse oximeters [1], brain tissue oximeter [2], optical imaging [3,4], photoacoustic oximetry [5,6], laser therapies [7], tattoo removal [8], and even the optical sensor on wearable devices [9]. As Battle and Hobbs noted, despite the limitations, laser procedures in pigmented skin are an open frontier with a growing demand [7]. Thus, a clear understanding of the interaction of light with human tissue in pigmented skins with a reproducible method is essential.

Currently, the Fitzpatrick color scale is widely used to categorize skin color. The Fitzpatrick color scale [10] classifies skin tone into 6 scales according to the skin's response to sun exposure, where type 1 corresponds to pale white skin and type 6 correspond to darker skin tones. The evaluation method consists of a self-classification questionnaire and clinical evaluation. However, the high subjectivity and low reproducibility of this method is known in the literature [11]. To avoid the limitations

of this method, Chardon *et al.* [12] developed an objective method of categorization using a numerical index, individual typology angle (ITA), which is obtained through colorimetric measurements with calibrated equipment.

To calculate the ITA values, a colorimeter or a spectrometer should access the $L^*a^*b^*$ color scale, which uses a three-dimensional color space to describe all colors perceived by the human eye. The L^* axis describes brightness/luminance, a^* is related to green and red colors, and b^* to blue and yellow. Recently, Bino and Bernerd [13] observed that the ITA is proportional to the concentration of skin pigments, and Zonios *et al.* [14] indicated that the concentration of melanin is linearly correlated with the ITA and can be estimated through [15]. Thus, it is possible to describe the constitutive properties of pigments only with the skin's colorimetric response.

Recently, it was shown that the optical properties (μ_a and μ'_s) of the skin are related to its color through ITA [16], and this information could be important in biomedical optics applications, as a correction factor for the fluence delivery in all skin phototypes. In this sense, this study aims to evaluate how skin color is correlated to its optical properties, suggesting

an experimental fitting method to access these optical properties using only the colorimetric response of the ITA, since it is a quantitative and reproducible method that indicates the concentration of pigments present in the skin.

2. MATERIALS AND METHODS

A. Colorimetric Measures

A colorimeter (Delta Vista 450G, Delta Color, Brazil) was employed to access the $L^*a^*b^*$ color scale of all the samples. The measurement was performed in triplicate, and the average was taken into consideration. By using the L^* and b^* measured values, it is possible to compute the individual typology angle (ITA) of the samples using the Eq. (1)

$$\text{ITA} = \frac{180}{\pi} \arctan \left(\frac{L^* - 50}{b^*} \right). \quad (1)$$

The ITA uses CIELAB colorimetric measurements to quantify and categorize the skin color according to its pigmentation as follows: very very light > 55° > light > 41° > intermediate > 28° > tan > 10° > brown > -30 > dark [12,13].

B. Optical Set-Up

A 3D-printed integrating sphere system and an RPS900-R spectrometer (International Light Technologies, USA) were employed to acquire the diffuse reflectance and transmittance from the human skin tissue. An SLS201 (Thorlabs, USA) light source was employed, providing a signal between 500 nm and 1300 nm. However, in this study, only the range from 500 nm up to 800 nm was analyzed, since we aim to correlate the samples' visible color and their optical properties. The inverse adding-doubling (IAD) method was used to compute the optical absorption and reduced scattering coefficient [17] through the experimental diffuse reflectance and transmittance. For detailed information about the system and measurement method, see reference [18]. As described in [16], we used refractive index $n = 1.40$ and anisotropic factor $g = 0.90$ to compute these optical properties using the IAD algorithm because these are the most common values for skin tissues [19]. However, the refractive index may vary between 1.41 and 1.49 for the epidermis and 1.36 to 1.41 for the dermis depending on the region analyzed, and the same may occur for the anisotropy factor, as described by Lister [20].

C. Ex vivo Human Skin Tissue

In this study, twelve *ex vivo* human skin tissues were optically analyzed. The samples were divided into six groups according to their ITA values, which can be seen in Table 1. The samples were acquired in collaboration with the Department of Plastic Surgery from the Ribeirão Preto Medical School of the University of São Paulo. Sample preparation for the optical measurement consisted of removing fat, blood, and fluids, leaving the dermis and epidermis intact. The measurements were performed within 3 h after surgery, maintaining the freshness of the samples and avoiding storage procedures that may change the optical properties of the samples [21]. The $L^*a^*b^*$ measurements were taken three times for each sample at the vicinity of the optical measurement spot. The mean and standard deviation were calculated taken into consideration the sample's group. The tissue thickness ranged from 1.69 mm up to 1.92 mm, but some fat residues may have been considered in the final thickness of each sample. All the samples have a lateral extent higher than 35 mm to avoid light losses during the experimental measures. All procedures were performed according to the ethical standards (Ethics Appreciation Certificate 0630218.2.0000.5440 and Approval Number 3.275.034).

The specimens used in this study are categorized into the intermediate, tan, and brown ITA typologies with values ranging from 32.7 to -13.5°. Despite covering only three categories, the samples maintain a wide range of 46.2°, encompassing a significant region of interest for skin tones and ensuring that it is possible to empirically derive the model proposed in this study.

3. RESULTS AND DISCUSSIONS

Figure 1 shows the skin tissue's absorption and reduced scattering coefficients dependence through wavelength, from 500 nm up to 800 nm. The average values are shown in solid lines and vertical bars correspond to the standard deviation.

The μ'_s in Fig. 1A decreases as the wavelength increases, and it remains similar for all sample groups. Our previous study [16] indicated that scattering did not significantly change with the ITA. On the other hand, the same study indicated that μ_a has a high dependence with the ITA values, where μ_a increases as the ITA decreases, as can be seen in Fig. 1B.

At 540 nm and 575 nm there are two hemoglobin (Hb) absorption bands [20]. Huang [22] showed that the a^* axis of the $L^*a^*b^*$ scale is directly related to the presence of blood, which Hb is its main absorber. Since the ITA does not use the a^* axis, the traces of Hb will not be considered in this study. The later analyses were made only for melanin absorption,

Table 1. Average and Standard Deviation of the $L^*a^*b^*$ Color Scale, ITA Values, and Skin Typology of the Six Abdominal Skin Sample Groups

No. Samples	L^*	a^*	b^*	ITA (degree)	Typology
5	60.7 ± 1.9	3.9 ± 0.9	16.4 ± 2.0	32.7 ± 0.6	Intermediate
2	59.5 ± 0.2	5.0 ± 1.2	17.3 ± 0.5	29.0 ± 0.4	Intermediate
1	56.7 ± 1.0	9.5 ± 0.8	16.3 ± 1.6	22.4 ± 0.9	Tan
2	57.6 ± 1.9	6.1 ± 1.2	22.3 ± 1.7	18.4 ± 0.8	Tan
1	48.5 ± 1.6	8.4 ± 0.3	20.8 ± 0.1	-4.2 ± 0.9	Brown
1	44.8 ± 0.7	10.5 ± 0.5	21.7 ± 0.7	-13.5 ± 0.7	Brown

4 134
135
136
137
138
139
140
141
142
143
144
145
146
147
148
149
150

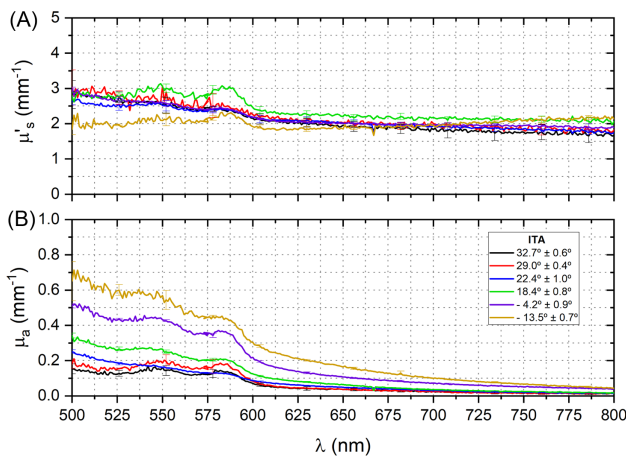


Fig. 1. A: Scattering and B: absorption coefficient of the skin tissue samples, labeled by ITA values.

which is the main pigmentation of the skin. In the near infrared region, human skins have water absorption bands at 970 nm and 1200 nm [19,23]. However, these values do not change for different ITA values [16]. This result was expected because the ITA is a numerical representation of the constitutive pigmentation of the skin [13], being suitable for an analysis in the visible region only.

Using the experimental data from Fig. 1, it is possible to make a change to the axis from the wavelength (λ) dependence to the ITA. Figure 2 shows the μ'_s and μ_a as a function of the ITA for several wavelengths, from 500 nm to 800 nm with a 10 nm spectral resolution and without the Hb range (530 nm up to 590 nm).

In Fig. 2A, the μ'_s at the ITA = -13.5° is much lower than that at the ITA = -4.2° , for 500–520 nm. This result was previously discussed in [16], being associated with a lower albedo range, which may not totally converge with some data

from the IAD method. The absorption coefficient in Fig. 2B is in logarithmic scale [$\log(\mu_a)$], which shows a possible linear relationship. The Hb bands ranging from 530 nm up to 590 nm at the μ_a was not taken into consideration, but all the data were considered for μ'_s .

A linear fitting, according to Eqs. (2) and (3), correlating μ'_s and μ_a with the ITA for several wavelengths, was made for both of them, and the result can be seen in Fig. 3,

$$\mu'_s = k_1 + k_2 \cdot \text{ITA}, \quad (2)$$

$$\log(\mu_a) = c_1 + c_2 \cdot \text{ITA}, \quad (3)$$

where k_1 , k_2 , c_1 , and c_2 are arbitrary model parameters. To ensure the mathematical adequacy, the model adapted μ_a to $\log(\mu_a)$ from the logarithmic scale used in Fig. 2.

As can be seen in Fig. 3A, all the μ'_s remained close to a constant region instead of a linear profile. This behavior was maintained for all wavelengths between 500 nm and 800 nm, including the Hb region. On the other hand, the linear fitting was able to successfully fit the absorption coefficient on a logarithmic scale. The linear fitting coefficient can be detailed, as seen in Fig. 4 for μ'_s and Fig. 5 for μ_a , over the entire spectra.

The k_2 parameter in Fig. 4 indicate that the slope term oscillates in the vicinity of zero for all wavelengths and has mean value of $k_2 = 0.000 \pm 0.004$. On the other hand, k_1 exhibit values close to the average μ'_s , indicating that it is possible to perform a linearization as a constant factor only. So we can simplify Eq. (2) to $\mu'_s = k_1$, since $k_2 \ll k_1$, confirming that μ'_s has no dependence on ITA for all λ from 500 to 800 nm.

While μ'_s parameters showed no correlation through the ITA, the opposite is true for μ_a . Figure 5B indicates a constant value for the fitting coefficient c_2 with a mean value of -0.014 ± 0.001 . However, the intercept c_1 changes linearly according to the λ and can be described by the Eq. (4) with a coefficient of determination $R^2 = 0.99$,

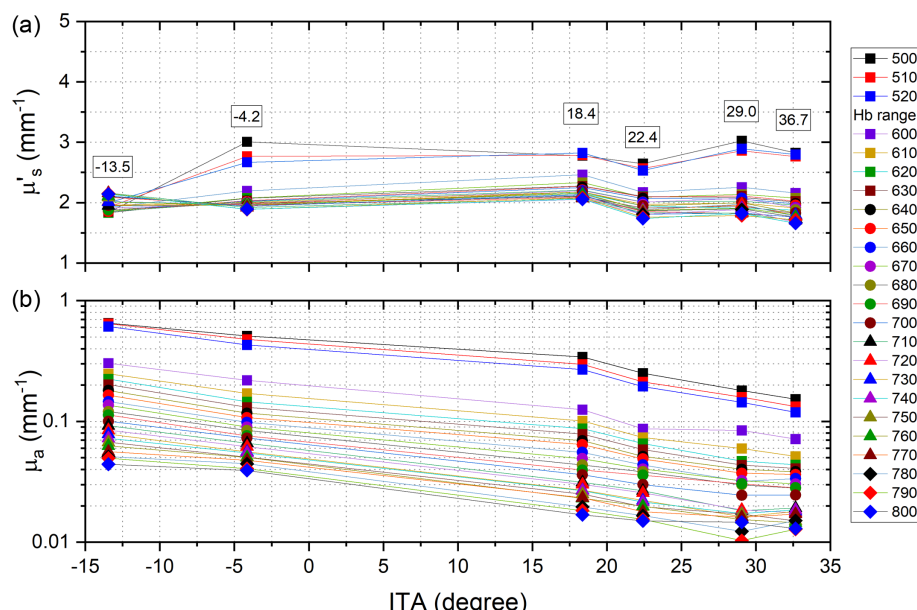


Fig. 2. (A) Scattering and (B) absorption coefficient dependence on the ITA values, from 500 nm up to 800 nm, with a 10 nm step. Hemoglobin range (630 nm until 690 nm) was not taken into consideration.

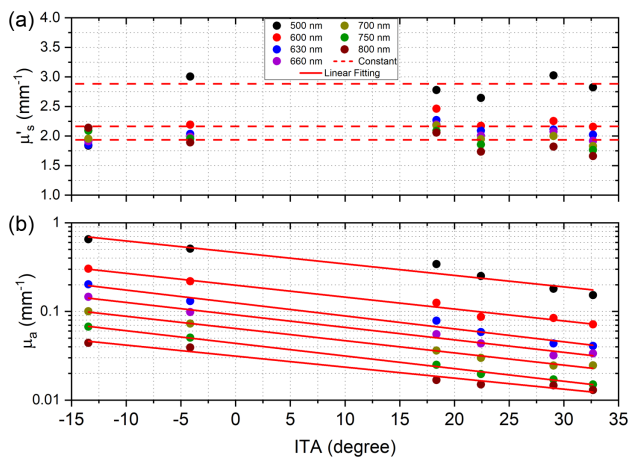


Fig. 3. Linear fitting of the optical parameters at 500 nm, 600 nm, 630 nm, 660 nm, 700 nm, 750 nm, and 800 nm. (A) The scattering and (B) absorption coefficient labeled by the ITA values.

$$c_1 = 1.657 - 0.004\lambda. \quad (4)$$

It is possible to set a relationship between μ_a as a function of the ITA. By using Eq. (3) and applying the exponential on $\log(\mu_a)$ to obtain μ_a in Eq. (5)

$$\mu_a = 10^{c_1} \cdot 10^{c_2 \cdot \text{ITA}}. \quad (5)$$

As shown in the previous section, c_2 has a constant value of -0.014 , and c_1 changes according to Eq. (4). These values can be substituted into Eq. (5),

$$\mu_a = 10^{1.657 - 0.004\lambda} \cdot 10^{-0.014 \cdot \text{ITA}}. \quad (6)$$

A readjustment in Eq. (6) can be performed, leading to Eq. (7),

$$\mu_a = 45.4 \cdot 10^{-0.004\lambda} \cdot 10^{-0.014 \cdot \text{ITA}}. \quad (7)$$

Equation (7) relates μ_a to the ITA values for all the λ within the visible range, except for the Hb range. Now, it is possible to estimate μ_a on *ex vivo* human skin solely by their ITA values and choosing the wavelength of interest. The λ is already in nm.

The μ'_s cannot be estimated using the same routine because it does not change according to the ITA values. However, it is well known in the literature that a general power law fitting [24] describes with good precision the μ'_s decay using λ by using Eq. (8):

$$\mu'_s = z_1 \left(\frac{\lambda}{500(\text{nm})} \right)^{-z_2}, \quad (8)$$

where z_1 and z_2 are amplitude and decay parameters from the power law equation. In this study, a 500 nm was used to normalize the power law equation. It can be chosen randomly but this value is preferred. Using the mean value from all μ'_s , we found the parameter $z_1 = 2.84 \pm 0.04$ and $z_2 = 1.03 \pm 0.06$ with $R^2 = 0.932$. Replacing them in Eq. (8) leads to Eq. (9) and fully describes the decreasing pattern of μ'_s with increasing λ ,

$$\mu'_s = 2.84 \cdot \left(\frac{\lambda}{500(\text{nm})} \right)^{-1.03}. \quad (9)$$

By using the ITA values presented in this study as reference to Eqs. (7) and (9), an experimental model of μ_a and μ'_s can be estimated and set side by side with the experimental values from Fig. 1. Figure 6 shows this comparison. As can be seen in Fig. 6, all the optical coefficients could be fitted. In both graphs, the μ'_s and μ_a indicate a compatibility with the experimental model, with R^2 between 0.932 and 0.997, except for the hemoglobin band ranges, which were disregarded in this study, indicating

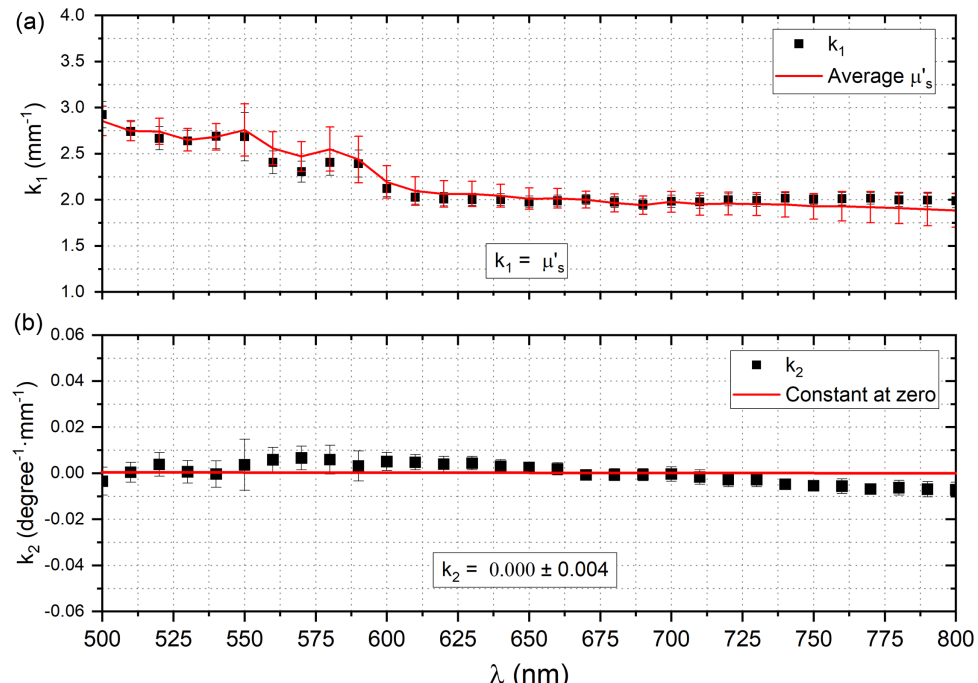


Fig. 4. Linear fitting parameters for the scattering coefficient. The slope k_2 oscillates in the vicinity of zero for all wavelengths and has mean value of 0.000 ± 0.004 . On the other hand, k_1 exhibit values close to the average μ'_s , indicating that we can make the linearization as a constant factor only.

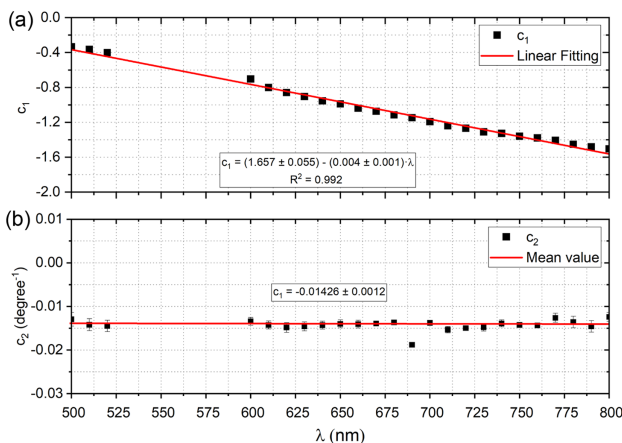


Fig. 5. (A) The intercept c_1 change linearly according to λ and can be described by the Eq. (4) with a coefficient of determination $R^2 = 0.99$. (B) Indicates a constant slope c_2 , with a mean value of -0.014 ± 0.001 .

a high suitability of the model proposed in this work with the experimental results.

Some spectral regions show higher deviation with the experimental model, but this could be related to experimental limitations. The μ_a of the sample ITA = 18.4° showed the higher discrepancy, and this result may be associated with the ITA measuring, since human skin's pigmentation is inhomogeneously distributed. The ITA is a relationship between the skin pigmentation and its color by using a numerical approach. Thus, our results are limited for the visible spectral range.

For dark skin (e.g., ITA = -13.45° in this study), it can be difficult to accurately measure μ'_s due to confounding effects from the high absorption of melanin in the epidermis. This limitation was also reported in a study using spatial

frequency domain imaging in different human phototypes, and the scattering coefficients were lower in higher Fitzpatrick scores [4].

Our results are valid for *ex-vivo* samples. In *in-vivo*, the optical and colorimetric properties may be different because there are more physiological interactions, since the constitutive pigmentation is set by biological regulations, such as melanoblasts migration, melanocytes density, enzymatic functions and expressions, melanin synthesis (eumelanin and pheomelanin), melanosomes transport, and melanin distribution. Also, toxic compounds, like hydroquinone, may also change the skin pigmentation [25]. However, the epidermal melanocytes slowly increase under normal circumstances and are resistant to apoptosis [26], indicating that the experimental fitting proposed in this study could be applied to evaluate the melanin solely in *in vivo* samples. This method is not suitable for hemoglobin bands, since it does not take the a^* parameter into consideration. Hyperpigmented skins were not studied in this paper, but in the future, it should be taken into consideration to confirm if the experimental model is still valid.

4. CONCLUSIONS

A correlation between the absorption and reduced scattering coefficients of *ex vivo* human skins were done through the individual typology angle using a numerical approach. The μ_a exhibited a direct relation with the ITA. This pattern could be described through an exponential equation, where the parameters were acquired through a linearization method. The μ'_s does not change with the ITA, but it could be described using a power law fitting. This experimental model will not work for hemoglobin bands and ranges other than the visible, and very high absorption coefficients do not adequately converge the IAD model and may limit the range of study using this

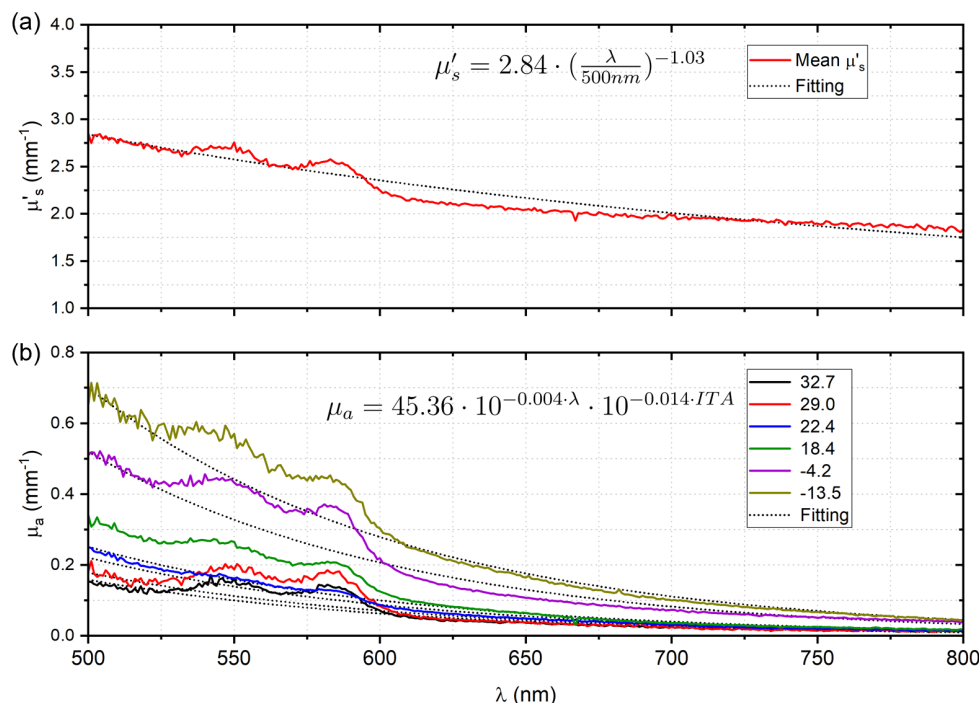


Fig. 6. Comparison between the experimental values and the fitting.

technique. Both optical coefficients could be determined with R^2 being higher than 0.93, indicating that the methodology is adequate and can estimate the optical parameters only with the ITA value of the skin. Lastly, while our study provides valuable insights into the absorption coefficient as a function of skin color, it is important to acknowledge that the calculated values were based on the literature mean g and n parameters, which were not specifically measured for the skin samples utilized in this research. Further investigations should involve a more diverse range of skin types to validate and expand comprehension of the results, which is a limitation of the current study, and by incorporating a layered model in the inverse adding-doubling analysis, which could also increase accuracy.

Funding. Fundação de Amparo à Pesquisa do Estado de São Paulo (2013/07276-1, 2017/25923-5, 2018/14955-6); Coordenação de Aperfeiçoamento de Pessoal de Nível Superior (001).

Acknowledgment. The authors thanks Cynthia Maria de Campos Prado Manso for the linguistic advice. The authors also thank the reviewers for their important contributions, which improved the manuscript.

All the authors made significant contributions to the manuscript. Pedro S. Coltro was the surgeon responsible for acquiring all the human tissue samples. Carlos E. Girasol was responsible for tissue collection, transportation, cleaning, and disposal. Luismar B. da Cruz Junior performed the optical measurements, characterization, and mathematical modeling. Luciano Bachmann and Rinaldo R. de Jesus supervised this work and made important intellectual contributions. All the authors approved the final version of the manuscript.

Ethics Approval. All the procedures were performed according to ethical standards and approved by the Ethics Committee of Hospital das Clínicas of the Ribeirão Preto Medical School from the University of São Paulo (Ethical Appreciation Certificate 0630218.2.0000.5440 and Approval Number 3.275.034).

Disclosures. The authors declare no conflicts of interest.

Data availability. Data underlying the results presented in this paper are not publicly available at this time but may be obtained from the authors upon reasonable request.

REFERENCES

- M. W. Sjoding, R. P. Dickson, T. J. Iwashyna, S. E. Gay, and T. S. Valley, "Racial bias in pulse oximetry measurement," *N. Engl. J. Med.* **383**, 2477–2478 (2020).
- P. E. Bickler, J. R. Feiner, and M. D. Rollins, "Factors affecting the performance of 5 cerebral oximeters during hypoxia in healthy volunteers," *Anesth. Analg.* **117**, 813–823 (2013).
- M. J. Mendenhall, A. S. Nunez, and R. K. Martin, "Human skin detection in the visible and near infrared," *Appl. Opt.* **54**, 10559–10570 (2015).
- T. Phan, R. Rowland, A. Ponticorvo, B. C. Le, R. H. Wilson, S. A. Sharif, G. T. Kennedy, N. P. Bernal, and A. J. Durkin, "Characterizing reduced scattering coefficient of normal human skin across different anatomic locations and Fitzpatrick skin types using spatial frequency domain imaging," *J. Biomed. Opt.* **26**, 026001 (2021).
- X. Li, U. S. Dinish, J. Aguirre, R. Bi, K. Dev, A. B. E. Attia, S. Nitkunanantharajah, Q. H. Lim, M. Schwarz, Y. W. Yew, S. T. G. Thng, V. Ntziachristos, and M. Olivo, "Optoacoustic mesoscopy analysis and quantitative estimation of specific imaging metrics in Fitzpatrick skin prototypes II to V," *J. Biophoton.* **12**, e201800442 (2019).
- Y. Mantri and J. V. Jokerst, "Impact of skin tone on photoacoustic oximetry and tools to minimize bias," *Biomed. Opt.* **13**, 875–887 (2022).
- E. F. Battle, Jr. and L. M. Hobbs, "Laser therapy on darker ethnic skin," *Dermatol. Clin.* **21**, P713–723 (2003).
- N. Khunger, A. Molpariya, and A. Khunger, "Complications of tattoos and tattoo removal: stop and think before you ink," *J. Cutan. Aesth. Surg.* **8**, 30–36 (2015).
- P. J. Colvon, "Response to: investigating sources of inaccuracy in wearable optical heart rate sensors," *NPJ Digit. Med.* **4**, 38 (2021).
- T. B. Fitzpatrick, "The validity and practicality of sun-reactive skin types I through VI," *Arch. Dermatol.* **124**, 869–871 (1988).
- C. E. Dubin, G. W. Kimmel, P. W. Hashim, J. K. Nia, and J. A. Zeichner, "Objective evaluation of skin sensitivity across Fitzpatrick skin types," *J. Drugs Dermatol.* **19**, 699–701 (2020).
- A. Chardon, I. Cretois, and C. Hourseau, "Skin colour typology and suntanning pathways," *Int. J. Cosmet. Sci.* **13**, 191–208 (1991).
- S. D. Bino and F. Bernerd, "Variations in skin colour and the biological consequences of ultraviolet radiation exposure," *Br. J. Dermatol.* **169**, 33–40 (2013).
- G. Zonios, J. Bykowski, and N. Kollias, "Skin melanin, hemoglobin, and light scattering properties can be quantitatively assessed *in vivo* using diffuse spectroscopy," *J. Invest. Dermatol.* **117**, 1452–1457 (2001).
- H. Wang, L. Jiang, C. Gao, X. Zhang, K. Xiao, M. Melgosa, and C. Li, "Skin color measurements before and after two weeks of sun exposure," *Vis. Res.* **192**, 107976 (2022).
- L. B. Cruz, Jr., C. Girasol, P. S. Coltro, R. R. J. Guiro, and L. Bachmann, "Optical properties of human skin phototypes and their correlation with individual angle typology," *Photobiomodul. Photomed. Laser Surg.* **41**, 175–181 (2023).
- S. A. Prahl, M. J. C. Gemert, and A. J. Welch, "Determining the optical properties of turbid media by using the adding-doubling method," *Appl. Opt.* **32**, 559–568 (1993).
- L. B. Cruz, Jr. and L. Bachmann, "Manufacture and characterization of a 3D-printed integrating sphere," *Instrum. Sci. Technol.* **49**, 276–287 (2020).
- A. N. Bashkatov, E. A. Genina, V. I. Kochubey, and V. V. Tuchin, "Optical properties of human skin, subcutaneous and mucous tissues in the wavelength range from 400 to 2000 nm," *J. Phys. D* **38**, 2543–2555 (2005).
- T. Lister, P. A. Wright, and P. H. Chappell, "Optical properties of human skin," *J. Biomed. Opt.* **17**, 090901 (2012).
- E. A. Genina, A. N. Bashkatov, V. I. Kochubey, and V. V. Tuchin, "Effect of storage conditions of skin samples on their optical characteristics," *Opt. Spectrosc.* **107**, 934–938 (2009).
- W.-S. Huang, Y.-W. Wang, K.-C. Hung, P.-S. Hsieh, K.-Y. Fu, L.-G. Dai, N.-H. Liou, K.-H. Ma, J.-C. Liu, and N.-T. Dai, "High correlation between skin color based on CIELAB color space, epidermal melanocyte ratio, and melanocyte melanin content," *PeerJ* **6**, e4815 (2018).
- E. Salomatina, B. Jiang, J. Novak, and A. N. Yaroslavsky, "Optical properties of normal and cancerous human skin in the visible and near-infrared spectral range," *J. Phys. D* **11**, 064026 (2006).
- S. L. Jacques, "Optical properties of biological tissue: a review," *Phys. Med. Biol.* **58**, R37–61 (2013).
- Y. Yamaguchi and V. J. Hearing, "Physiological factors that regulate skin pigmentation," *Biofactors* **35**, 193–199 (2009).
- Y. Yamaguchi, M. Brenner, and V. J. Hearing, "The regulation of skin pigmentation," *J. Biol. Chem.* **282**, 27557–27561 (2007).

278	and quantitative estimation of specific imaging metrics in Fitzpatrick skin phototypes II to V," <i>J. Biophoton.</i> 12 , e201800442 (2019).	330
279	6. Y. Mantri and J. V. Jokerst, "Impact of skin tone on photoacoustic	331
280	oximetry and tools to minimize bias," <i>Biomed. Opt.</i> 13 , 875–887	332
281	(2022).	333
282	7. E. F. Battle, Jr. and L. M. Hobbs, "Laser therapy on darker ethnic	334
283	skin," <i>Dermatol. Clin.</i> 21 , P713–723 (2003).	335
284	8. N. Khunger, A. Molpariya, and A. Khunger, "Complications of tattoos	336
285	and tattoo removal: stop and think before you ink," <i>J. Cutan. Aesth.</i>	337
286	<i>Surg.</i> 8 , 30–36 (2015).	338
287	9. P. J. Colvon, "Response to: investigating sources of inaccuracy in	339
288	wearable optical heart rate sensors," <i>NPJ Digit. Med.</i> 4 , 38 (2021).	340
289	10. T. B. Fitzpatrick, "The validity and practicality of sun-reactive skin	341
290	types I through VI," <i>Arch. Dermatol.</i> 124 , 869–871 (1988).	342
291	11. C. E. Dubin, G. W. Kimmel, P. W. Hashim, J. K. Nia, and J. A. Zeichner,	343
292	"Objective evaluation of skin sensitivity across Fitzpatrick skin	344
293	types," <i>J. Drugs Dermatol.</i> 19 , 699–701 (2020).	345
294	12. A. Chardon, I. Cretois, and C. Hourseau, "Skin colour typology and	346
295	suntanning pathways," <i>Int. J. Cosmet. Sci.</i> 13 , 191–208 (1991).	347
296	13. S. D. Bino and F. Bernerd, "Variations in skin colour and the biological	348
297	consequences of ultraviolet radiation exposure," <i>Br. J. Dermatol.</i>	349
298	169 , 33–40 (2013).	350
299	14. G. Zonios, J. Bykowski, and N. Kollias, "Skin melanin, hemoglobin,	351
300	and light scattering properties can be quantitatively assessed <i>in vivo</i>	352
301	using diffuse spectroscopy," <i>J. Invest. Dermatol.</i> 117 , 1452–1457	353
302	(2001).	354
303	15. H. Wang, L. Jiang, C. Gao, X. Zhang, K. Xiao, M. Melgosa, and C. Li,	355
304	"Skin color measurements before and after two weeks of sun exposure," <i>Vis. Res.</i> 192 , 107976 (2022).	356
305	16. L. B. Cruz, Jr., C. Girasol, P. S. Coltro, R. R. J. Guiro, and L.	357
306	Bachmann, "Optical properties of human skin phototypes and	358
307	their correlation with individual angle typology," <i>Photobiomodul.</i>	359
308	<i>Photomed. Laser Surg.</i> 41 , 175–181 (2023).	360
309	17. S. A. Prahl, M. J. C. Gemert, and A. J. Welch, "Determining the optical	361
310	properties of turbid media by using the adding-doubling method," <i>Appl. Opt.</i>	362
311	32 , 559–568 (1993).	363
312	18. L. B. Cruz, Jr. and L. Bachmann, "Manufacture and characterization	364
313	of a 3D-printed integrating sphere," <i>Instrum. Sci. Technol.</i> 49 ,	365
314	276–287 (2020).	366
315	19. A. N. Bashkatov, E. A. Genina, V. I. Kochubey, and V. V. Tuchin,	367
316	"Optical properties of human skin, subcutaneous and mucous tissues	368
317	in the wavelength range from 400 to 2000 nm," <i>J. Phys. D</i> 38 ,	369
318	2543–2555 (2005).	370
319	20. T. Lister, P. A. Wright, and P. H. Chappell, "Optical properties of	371
320	human skin," <i>J. Biomed. Opt.</i> 17 , 090901 (2012).	372
321	21. E. A. Genina, A. N. Bashkatov, V. I. Kochubey, and V. V. Tuchin,	373
322	"Effect of storage conditions of skin samples on their optical	374
323	characteristics," <i>Opt. Spectrosc.</i> 107 , 934–938 (2009).	375
324	22. W.-S. Huang, Y.-W. Wang, K.-C. Hung, P.-S. Hsieh, K.-Y. Fu, L.-G.	376
325	Dai, N.-H. Liou, K.-H. Ma, J.-C. Liu, and N.-T. Dai, "High correlation	377
326	between skin color based on CIELAB color space, epidermal	378
327	melanocyte ratio, and melanocyte melanin content," <i>PeerJ</i> 6 ,	379
328	e4815 (2018).	380
329	23. E. Salomatina, B. Jiang, J. Novak, and A. N. Yaroslavsky, "Optical	381
330	properties of normal and cancerous human skin in the visible and	382
331	near-infrared spectral range," <i>J. Phys. D</i> 11 , 064026 (2006).	383
332	24. S. L. Jacques, "Optical properties of biological tissue: a review," <i>Phys. Med. Biol.</i>	384
333	58 , R37–61 (2013).	385
334	25. Y. Yamaguchi and V. J. Hearing, "Physiological factors that regulate	386
335	skin pigmentation," <i>Biofactors</i> 35 , 193–199 (2009).	387
336	26. Y. Yamaguchi, M. Brenner, and V. J. Hearing, "The regulation of skin	388
337	pigmentation," <i>J. Biol. Chem.</i> 282 , 27557–27561 (2007).	389
338		390
339		391